Available online at www.sciencedirect.com
SCIENCE DIRECT®
Journal of Crystal Growth 261 (2004) 359–363
JOURNAL OF CRYSTAL GROWTH
www.elsevier.com/locate/jcrysgro

Characteristics of stable emission GaN-based resonant-cavity light-emitting diodes

C.F. Lin*, H.H. Yao, J.W. Lu, Y.L. Hsieh, H.C. Kuo, S.C. Wang

Institute of Electro-optical Engineering, National Chiao Tung University, Hsinchu 300, Taiwan, ROC

Abstract

The resonant-cavity light-emitting diode (RC-LED) structure was grown by MOCVD. The structure of RC-LED consisted of a 3λ InGaN/GaN MQW LED cavity between the top TiO_2/SiO_2 DBR (81.7%, reflectance) and the bottom AlN/GaN DBR (90.4%) stack. A stable 410 nm emission peak and a low thermally induced red-shift effect (0.12 nm/kA/cm^2) were measured by varying the injection current density. The light output power of the full RC-LED device was three times higher than the RC-LED without top TiO_2/SiO_2 DBR layers under 600 A/cm^2 inject current density. The narrow line width of 7.4 nm, emission peak localization at 410 nm, and three times higher output power were caused by the resonance effect in this vertical cavity structure.

PACS: 81.15.Gh; 85.60.Bt; 85.60.Jb

Keywords: A3. Metalorganic chemical vapor deposition; B2. AlN/GaN; B2. Distributed Bragg reflectors; B2. GaN; B2. InGaN/GaN; B3. Resonant-cavity light-emitting diode

1. Introduction

Gallium nitride is a direct wide band gap semiconductor, which has attracted great attention for application to light sources of short wavelength. In particular, GaN-based semiconductor laser diodes (LDs) and light emitting diodes (LEDs) have applications in displays, traffic signals, and high density DVDs. Although there are still many issues in blue edge emitting LDs and LEDs, the research interest has gradually shifted to the development and demonstration of GaN-based vertical cavity surface emitting lasers (VCSELs) [1–4] and resonant-cavity light-emitting diodes (RC-LEDs) [5–10]. An important requirement for the operation of such devices is the use of high reflectance mirrors, usually in the form of distributed Bragg reflectors (DBRs). The VCSELs require highly reflective DBR mirrors on both sides of the active region to form the resonant cavity; while for the RCLEDs, the high reflectance DBRs can improve the output power and emission spectrum.

The DBR structures are particularly important for GaN VCSELs in two respects. The first aspect is the high reflectivity. According to Honda and co-workers, the threshold current density of a GaN VCSEL [11] can be reduced by an order of

*Corresponding author. Tel.: +886-3-5712121-56327; fax: +886-3-5716631.
E-mail address: cfjlin@ms32.hinet.net (C.F. Lin).

0022-0248/$ - see front matter © 2003 Published by Elsevier B.V.
doi:10.1016/j.jcrysgro.2003.11.028

magnitude with an increase of the DBR peak reflectance from 90% to 99%. The second aspect is the large stopband width. This is important because the active region of the GaN based VCSEL is typically made of InGaN multiple quantum wells (MQWs), and the emission spectrum of the InGaN MQWs tends to fluctuate with small variations in growth or process parameters [12–14]. Therefore, the wide stopband of the DBRs allows coverage of such spectral variation.

Several GaN/AlGaN based DBR structures have been reported, grown either by molecular beam epitaxy (MBE) [15–17] or by metal organic chemical vapor deposition (MOCVD) [18–20]. In order to reduce the number of pairs and increase the mirror stopband, the use of materials with high index of refraction contrast such as AlN/GaN is desirable and was reported using MBE and MOCVD [21–24]. Using plasma-assisted MBE, Ng et al. [22] reported a peak reflectance of up to 99% centered at 467 nm with a bandwidth of 45 nm, and demonstrated that the network of cracks on AlN/GaN DBR can be reduced or completely eliminated by the use of asymmetric DBR structures [22]. The highest peak reflectance for MOCVD grown AlN/GaN DBR structures is only about 88% [24].

In this paper, the epitaxial growth, device fabrication, and performance of GaN-based RC-LEDs are discussed. The stability, localization, and higher output power of the electroluminescence are also discussed in detail for this vertical resonance cavity.

2. Experiments

The blue RC-LED structures were grown in a metal-organic chemical vapor deposition (MOCVD) System (EMCORE D-75) on polished optical-grade C-face (0001) 2″ diameter sapphire substrates. The sapphire substrate was placed on a graphite susceptor with a filament heater in the vertical type reactor. Trimethylgallium (TMGa), Trimethylaluminum (TMAl), and ammonia (NH_3) were used as the Ga, Al and N sources, respectively. The chamber pressure was fixed at 100 Torr. After growing a first GaN nucleation layer at 530°C, the temperature was raised to 1040°C to grow a buffer layer of undoped GaN (HT-GaN). Then the 20 pairs AlN/GaN DBR was deposited on the undoped GaN bulk layer. The 3λ cavity of the RC-LED structure consisted of a GaN:Si n-type region, ten pairs of InGaN/GaN MQW layers as the active layer, and a GaN:Mg p-type layer. In the RC-LED structure, the 20 pairs AlN/GaN DBR was grown below the MQW active layer as the high reflectivity mirror. The reflectance of the AlN/GaN DBR structure was measured by an n&k ultraviolet-visible spectrometer with normal incidence at room temperature. The Ti/Al and Ni/Au metals were deposited as the n-type and p-type metal. A patterned SiO_2 layer was deposited as the current confinement layer defining the aperture region on the mesa region. Finally, two pairs, TiO_2/SiO_2 dielectric DBR was deposited as the top mirror to fabricate the RCLED device. The PL and EL emission spectra of the LED and RC-LED structures were measured by a PL system with a He–Cd laser and an Alpha-SNOM system. The Alpha-SNOM system can function as a scanning near-field optical microscope to analyze the micro-optical properties of the VCSELs. The SNOM system is used to analyze the output mode and near-field pattern of VCSEL emission.

3. Results and discussion

The PL and X-ray spectra of the conventional LED structure with 10 periods InGaN/GaN MQW active layer were measured and are shown in Fig. 1. The PL peak of the InGaN/GaN MQW LED was located at 410.2 nm with an 18 nm line width. In Fig. 1(a), the PL spectrum clearly shows small oscillations caused by optical interference effects. This appearance of Fabry-Perot fringes indicated the smooth surface and uniform interfaces of the InGaN/GaN MQW-LED structures. In the DCX-ray rocking curve, shown in Fig. 1(b), the GaN, the InGaN peak, and one satellite peak are clearly observed, which shows the good quality of the GaN/InGaN interfaces and calculated the GaN/InGaN MQW property. The average In content and pair thickness were calculated as 6%

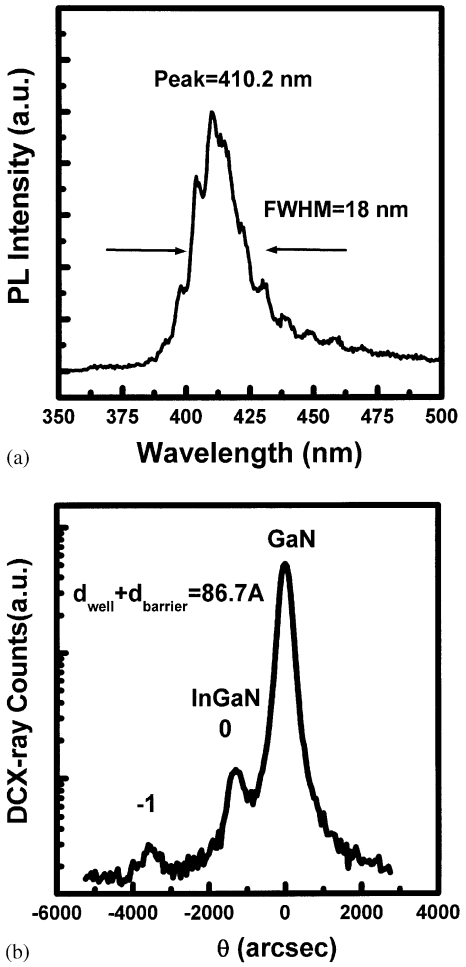

Fig. 1. PL spectrum and DCX-ray spectra of GaN/InGaN MQW structure.

and 86.7 Å in the InGaN/GaN MQW LED structure. This InGaN/GaN MQW active region was used in the RC-LED structure. The RC-LED structure consisted of the GaN buffer layer, undoped GaN layer, 20 pairs AlN/GaN DBR, and the 3λ cavity of LED structure. The reflectance spectrum of the 20 pairs AlN/GaN DBR structure is shown in Fig. 2. The peak reflectance is located at 410 nm with 90.4% reflectivity and 22 nm stopband width. The 3λ cavity, consisting of the GaN:Si n-type layer, InGaN/GaN MQW active layer, and GaN:Mg p-type layer was grown on the AlN/GaN DBR structure.

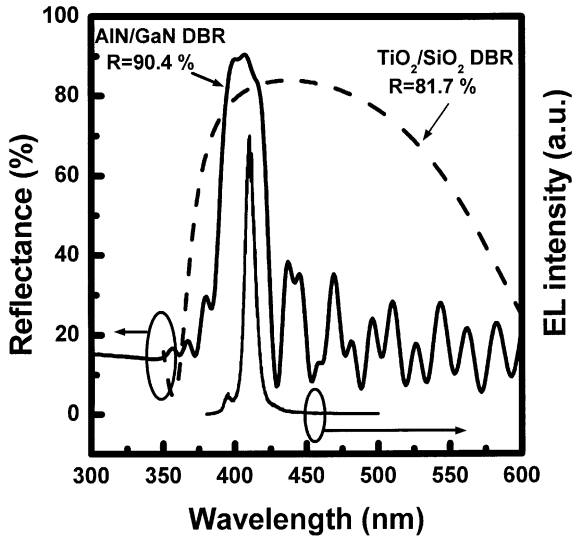

Fig. 2. Reflectance of 2-pairs TiO_2/SiO_2 DBR and 20-pairs AlN/GaN bottom DBRas measured by the n&k ultraviolet–visible spectrometer. The EL emission spectrum was located at 410 nm in this vertical cavity structure.

To compare the emission spectra of conventional LED and RC-LED structure, the PL emission peaks of both LED samples were measured at RT. The PL emission peak of the conventional LED structure was located at 410.2 nm with 18 nm line width as shown in Fig. 1(a). The emission peak of the RC-LED was located at 410 nm; this result indicates that the bottom AlN/GaN DBR did not have induced emission shift due to strain.

In order to confine the injection current to the aperture region, a 300 nm-thick SiO_2 layer was deposited at the mesa region with the 20 μm open aperture. A thin Ni/Au bilayer (with 50 Å/50 Å-thick) was deposited on the open aperture region for current spreading. The top 2-pairs and $\lambda/4$ stack of TiO_2/SiO_2 DBR layers were deposited on the RC-LED sample by e-gun evaporation, their thicknesses being controlled by a quartz monitor. The reflectance of the TiO_2/SiO_2 DBR layer on the spectrum monitoring quartz substrate is shown in Fig. 2. In order to measure the EL spectrum from the top surface of the RC-LED, a lower reflectivity TiO_2/SiO_2 stack (81.7%) was deposited on the aperture region. The reflectance of the 2-pairs

TiO_2/SiO_2 DBR was lower than that of the 20-pairs AlN/GaN bottom DBR structure (90.4%) at 410 nm. After the full vertical cavity RC-LED structure was fabricated, its EL emission spectrum by the SNOM system as a function of the injection current (Fig. 2). The typical EL emission peak was located at 410 nm, which coincides with the high reflectivity region of the top TiO_2/SiO_2 and the bottom AlN/GaN DBR structure. The line width of the EL emission peak was narrowed from 12.5 nm (with bottom AlN/GaN DBR) to 7.4 nm (with top TiO_2/SiO_2 and bottom AlN/GaN DBR). Because of the optical confinement of top and bottom DBR structure, the EL emission peak was fixed in this optical vertical cavity structure. The line width narrowing and emission peak localization were caused by the resonance effect in this vertical cavity structure.

The wavelength of EL emission as a function of injection current density is shown in Fig. 3. The EL emission peak of a RC-LED without top TiO_2/SiO_2 DBR layers has a stronger red shift of 0.48 nm/kA/cm^2 due to the thermal heating effect under higher current density. A red shift of 0.12 nm/kA/cm^2 is measured in the full RC-LED device by varying the injection current. This stability of the EL wavelength was caused by the cavity effect with the resonant cavity Fabry-Perot dip.

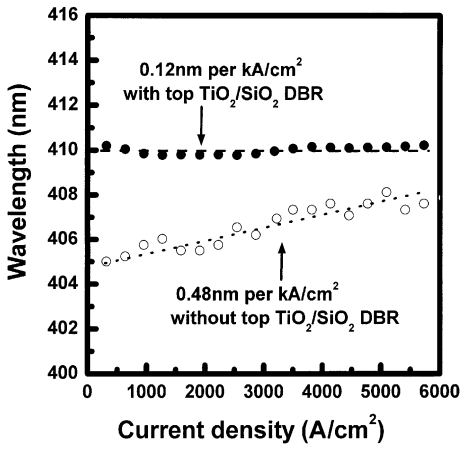

Fig. 3. The EL emission spectrum of the RC-LEDs with and without top TiO_2/SiO_2 DBR, measured at different injection current densities.

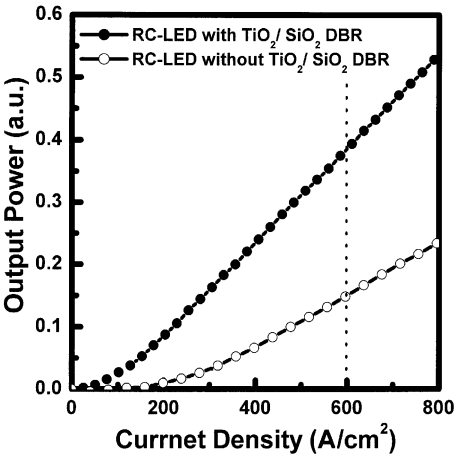

Fig. 4. Comparison of the output power of the RC-LEDs with and without top TiO_2/SiO_2 DBR at different injection current densities.

The output power as a function of injection current density is shown in Fig. 4. Compared the output powers at 600 A/cm^2 injection current density, the intensity of the RC-LED was three times higher than the RC-LED without top TiO_2/SiO_2 DBR layers. This output power increase was caused by the vertical resonant cavity effect and the directional light emission.

4. Conclusions

In conclusion, 3λ GaN-based LED vertical resonant cavity RC-LED structures were grown by MOCVD. In RC-LED structures, the 3λ InGaN/GaN MQW resonant cavities have been grown between the top TiO_2/SiO_2 DBR and the bottom AlN/GaN DBR stack. For measuring the EL spectrum from the top surface issue, lower reflectivity top TiO_2/SiO_2 DBR (81.7%) and higher reflectivity bottom AlN/GaN DBR (90.4%) were deposited on the aperture region. From the EL measurement of the RC-LED, the emission peak is 410 nm with low red-shift property of 0.12 nm/kA/cm^2 with injection current density. The line width narrowing effect, emission peak localization at 410 nm, and three times higher output power under 600 A/cm^2 injection current

density were caused by the resonance effect in this vertical cavity structure. Compared to the LEDs, the RC-LEDs exhibit much less red-shifting with injection current and a higher output power. Such RC-LEDs could be used as basis for GaN-based VCSELs.

Acknowledgements

This research was supported by the National Science Council of Taiwan, ROC, under the Contract No., NSC 92-2215-E-009-015 and NSC 92-2120-M-009-006. And by the Ministry of Education of Taiwan, ROC under the contract No. 88-FA06-AB.

References

[1] Tohru Honda, Atsushi Katsube, Takahiro Sakaguchi, Fumio Koyama, Kenichi Iga, Jpn. J. Appl. Phys., Part 1 24 (1995) 3527.
[2] Joan M. Redwing, David A.S. Loeber, Neal G. Anderson, . Michael A, Jeffrey S. Tischler, Flynn, Appl. Phys. Lett. 69 (1996) 1.
[3] Takao Someya, Koichi Tachibana, Jungkeun Lee, Takeshi Kamiya, Yasuhiko Arakawa, Jpn. J. Appl. Phys., Part 2 37 (1998) 1424.
[4] I.L. Krestnikov, W.V. Lundin, A.V. Sakharov, V.A. Semenov, A.S. Usikov, A.F. Tsatsul'nikov, Zh.I. Alferov, N.N. Ledentsov, A. Hoffmann, D. Bimberg, Appl. Phys. Lett. 75 (1999) 1192.
[5] Y.-K. Song, H. Zhou, M. Diagne, I. Ozden, A. Vertikov, A.V. Nurmikko, C. Carter-Coman, R.S. Kern, F.A. Kish, M.R. Krames, Appl. Phys. Lett. 74 (1999) 3441.
[6] Y.-K. Song, M. Diagne, H. Zhou, A.V. Nurmikko, C. Carter-Coman, R.S. Kern, F.A. Kish, M.R. Krames, Appl. Phys. Lett. 74 (1999) 3720.
[7] Y.-K. Song, M. Diagne, H. Zhou, A.V. Nurmikko, R.P. Schneider Jr., T. Takeuchi, Appl. Phys. Lett. 77 (2000) 1744.
[8] N. Nakada, M. Nakaji, H. Ishikawa, T. Egawa, M. Umeno, T. Jimbo, Appl. Phys. Lett. 76 (2000) 1804.
[9] S. Fern'andez, F.B. Naranjo, F. Calle, M.A. S'anchez-Garc'ỳa, E. Calleja, P. Vennegues, A. Trampert, K.H. Ploog, Semicond. Sci. Technol. 16 (2001) 913.
[10] F.B. Naranjo, S. Ferna'ndez, M.A. Sa'nchez-Garcỳ'a, F. Calle, E. Calleja, Appl. Phys. Lett. 80 (2002) 2198.
[11] T. Honda, A. Katsube, T. Sakaguchi, F. Koyama, K. Iga, Jpn. J. Appl. Phys., Part 1 34 (7A) (1995) 3527.
[12] H.M. Ng, T.D. Moustakas, S.N.G. Chu, Appl. Phys. Lett. 76 (20) (2000) 281.
[13] R. Singh, D. Doppalapudi, T.D. Moustakas, L.T. Romano, Appl. Phys. Lett. 70 (9) (1997) 1089.
[14] D. Doppalapudi, S.N. Basu, T.D. Moustakas, J. Appl. Phys. 85 (2) (1999) 883.
[15] R. Langer, A. Barski, J. Simon, N.T. Pelekanos, O. Konovalov, R. Andre, Le Si Dang, Appl. Phys. Lett. 74(24) (1999) 3610.
[16] S. Fernandez, F.B. Naranjo, F. Calle, M.A. Sanchez-Garcia, E. Calleja, P. Vennegues, A. Trampert, K.H. Ploog, Appl. Phys. Lett. 79 (14) (2001) 2136.
[17] F. Natali, D. Byrne, A. Dussaigne, N. Grandjean, J. Massies, B. Damilano, Appl. Phys. Lett.. 82 (4) (2003) 499.
[18] T. Someya, Y. Arakawa, Appl. Phys. Lett. 73 (25) (1998) 3653.
[19] K.E. Waldrip, J. Han, J.J. Figiel, H. Zhou, E. Makarona, A.V. Nurmikko, Appl. Phys. Lett. 78 (21) (2001) 3205.
[20] H.P.D. Schenk, P. de Mierry, P. Vennegues, O. Tottereau, M. Laugt, M. Vaille, E. Feltin, B. Beaumont, P. Gibart, S. Fernandez, F. Calle, Appl. Phys. Lett. 80 (2) (2002) 174.
[21] I.J. Fritz, T.J. Drummond, Electronics Letters 31 (1) (1995) 68.
[22] H.M. Ng, T.D. Moustakas, S.N.G. Chu, Appl. Phys. Lett. 76 (20) (2000) 2818.
[23] Franck Natali, Nadège Antoine-Vincent, Fabrice Semond, Declan Byrne, Lionel Hirsch, Albert Serge Barrière, Mathieu Leroux, Jean Massies, Joel Leymarie, Jpn. J. Appl. Phys., Part 2 41 (2002) 1140.
[24] T. Shirasawa, N. Mochida, A. Inoue, T. Honda, T. Sakaguchi, F. Koyama, K. Iga, J. Crystal Growth 189–190 (1998) 124.